Journal of Geochemical Exploration 182 (2017) 53–69

Contents lists available at ScienceDirect

Journal of Geochemical Exploration

journal homepage: www.elsevier.com/locate/gexplo

The long-term interaction of mine tailings with soils and the wider environment: Examples from Mont Chemin, Switzerland

Markus Egli[a,*], Annelies Berger[e], Rainer Kündig[b,c], Rolf Krebs[d], Raquel de Castro Portes[a], Roman Berger[d], Roger Widmer[b]

[a] Department of Geography, University of Zurich, Switzerland
[b] Swiss Geotechnical Commission, Department of Earth Sciences, ETH Zürich, Switzerland
[c] NEROS, Netzwerk Mineralische Rohstoffe Schweiz, Switzerland
[d] Institute of Natural Resource Sciences, Zurich University of Applied Sciences, Wädenswil, Switzerland
[e] Wanner AG, Solothurn, Switzerland

ARTICLE INFO

Keywords:
Element leaching
Weathering
Mine tailing
Soil
Chronosequence
Alps

ABSTRACT

There is no doubt that mine tailings and waste are an environmental problem and can be a risk to human health and other organisms. Although many studies about acid rock drainage have been performed, the dispersal of trace elements and their impact on the environment (groundwater, soils and agricultural use) and the long-term (i.e., decades to centuries) behaviour of mine tailings on silicate parent rock is still a matter of debate. Our main scope was, therefore, to develop an approach that enables a relatively fast and reliable prediction of the leaching of potentially toxic elements and, thus, to determine the reactivity of former mining sites. To do so, we traced back the leaching behaviour of metals such as copper (Cu), chromium (Cr), cadmium (Cd) and lead (Pb) in soils formed on tailings from small mines over a relatively long time period. Using a chronosequence approach based on historical records of mining activities and C-14 dating, element leaching could be traced over a time period of approximately 1000 years for the historic mining sites at Mont Chemin (Switzerland). The weathering index B, that expresses chemical leaching of base cations and weathering of silicate minerals, and trace element ratios to immobile compounds (such as hafnium (Hf)) indicated that element leaching, and thus reactivity of the material, was very intense during the first 200 years after abandonment of the site. Between approximately 200–400 years, the rate of elemental change in the soils was strongly reduced tending (moderate reactivity) to very small values, and consequently low reactivity, for exposure ages of > 400 years. Thus, the chronosequence approach enabled to determine the reactivity of the sites. Soil organic carbon and oxyhydroxides were not effective enough to completely retain trace metals. Many former small mining sites exist in the Swiss Alps. Using a database that contains information about the period of activity, date of abandonment, elements used and geology, we extrapolated our findings to sites in Switzerland with moderately comparable conditions to Mont Chemin. This relatively simple empirical approach enabled a spatialisation and rough estimation of the sites regarding their reactivity. A large number of small mining sites in Switzerland were characterised as still highly reactive and only a few were considered to be weakly reactive. With the help of the chronosequence approach and extrapolation of the small former mining sites, a relatively fast overview of the reactivity of sites could be achieved. This approach, however, cannot substitute for a detailed risk analysis of such sites.

1. Introduction

Bedrock lithology, ore occurrences and human contamination all have an influence on the element concentrations in soils and consequently in plants (e.g. Reimann et al., 2007). The major external source of trace metals in soils is usually contamination caused by anthropogenic activities, such as metal mining, smelting and processing or the use of fossil fuels. It is well known that mining and processing of metal ore can be significant causes of trace metal contamination of the environment (Dudka and Adriano, 1997; Egli et al., 2011a; Kim and Hyun, 2015; Navarro et al., 2008; Singh et al., 2005; Zhuang et al., 2009). Mine sites may be a potential threat to public health due to the risk of polluting nearby groundwater, soils, livestocks and crops, unless managed properly, because high concentrations of trace metals and metalloids can be discharged from mine waste (e.g., mine debris and mine-impacted soils) (Bech et al., 2017; Duruibe et al., 2007). The

* Corresponding author.
E-mail address: markus.egli@geo.uzh.ch (M. Egli).

http://dx.doi.org/10.1016/j.gexplo.2017.08.011
Received 27 March 2017; Received in revised form 2 August 2017; Accepted 27 August 2017
Available online 31 August 2017
0375-6742/

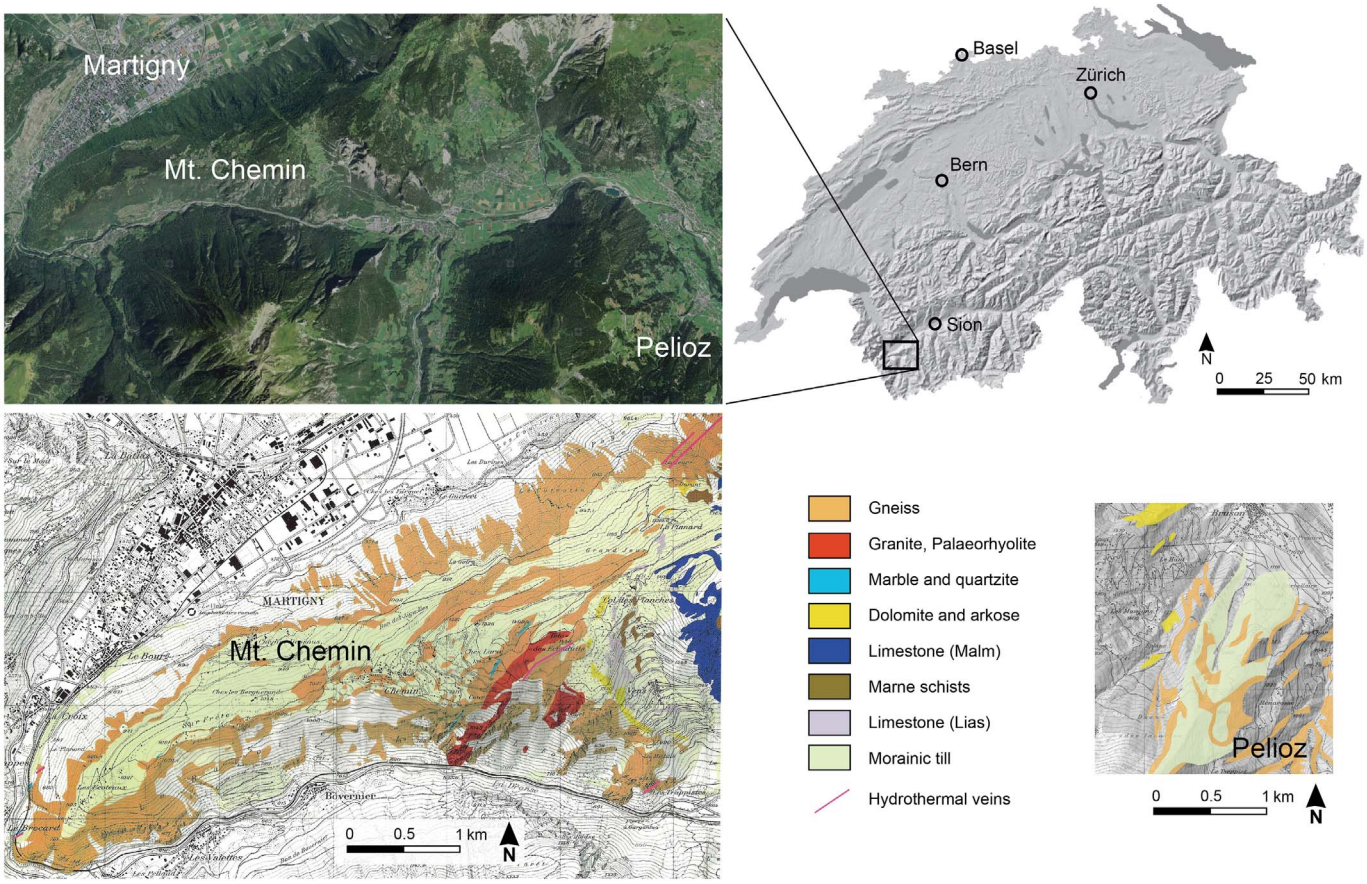

Fig. 1. Overview and geological settings of the investigation area Mt. Chemin (Ansermet, 2001. Reproduced by permission of swisstopo (BA17094).

environmental concern in mining areas is related to physical disturbance of the surrounding landscape (Dennis et al., 2003; Strosnider et al., 2007), spilled mine tailings, emitted dust (aeolian mobilisation) and mine drainage transported into surface and groundwater.

Plant effluents that are directly connected to rivers may cause (particularly during flood events) widespread disruption and significant damage to property (Dennis et al., 2003; Strosnider et al., 2007). Processing and combustion of sulphide bearing materials may lead to an increased emission of volatile elements such as Arsenic (Bortnikova et al., 2017). Excessive accumulation of trace metals in agricultural soils around mining areas, resulting in elevated trace metal uptake by food crops, is of great concern because of the potential health risk to local inhabitants. Fortunately, most occurrences are far away from civilisation.

The mined minerals are often sulphides or carbonates and are therefore highly reactive when coming into contact with atmospheric conditions (oxygen) and water. This gives rise to AMD (acid mine drainage) and BMD (basic mine drainage; e.g., Arefieva et al., 2016). Lead and zinc, for example, are predominantly derived from galena (PbS) and sphalerite (ZnS). Also Fe-S forms are often a by-product in exploited mines. Weathering of sulphides includes oxidation of sulphur and, in the presence of water, the production of sulphuric acid. The reaction is abiotically and biotically catalysed (e.g., Lawrence et al., 1997). For sphalerite, this gives

$$ZnS + 2O_2 + 2H_2O = Zn(OH)_2 + H_2SO_4 \quad (1)$$

and for the more frequently occurring pyrite and FeS:

$$FeS_2(s) + 15/4O_2 + 5/2H_2O = FeOOH(s) + 2SO_4^{2-} + 4H^+$$
$$FeS(s) + 9/4O_2 + 3/2H_2O = FeOOH(s) + SO_4^{2-} + 2H^+ \quad (2)$$

The extraction of metals from sulphide minerals results in large amounts of waste materials, tailings, and acid mine drainages giving rise to the transfer of potential toxic elements (e.g., As, Cu, Zn and Cd as examples) to the pedosphere and biosphere (Candeias et al., 2014). Therefore, water draining from such mines frequently contains high levels of sulphuric acid and trace metals (Lin et al., 2007; Shu et al., 2001), which could contaminate drinking water or agricultural lands when the mine water or mine water-affected stream water is used for irrigation purposes (e.g., Garcia-Guinea and Harffy, 1998; Strosnider et al., 2007).

Since the Bronze Age, metals have been exploited in the European Alpine arc: the majority used in the Late Bronze age were metals from the Alps (McIntosh, 2006). Iron became exploited in approximately 1000 BCE, and over the entire Alpine arc, mining activities have existed. In some areas, the amount and quality is sufficiently high for continuous exploitation. However, Switzerland, as a typical Alpine country, is rich in 'poor mines'. Although Switzerland has mineral resources, their quantity and quality have been too low for extensive exploitation over a longer duration. Furthermore, such sites are often difficult to assess. As a consequence, approximately 100 mines all over Switzerland have existed – but mostly only for a quite restricted time period. Due to economic reasons, almost no mining activities (with the exception of bulk materials) currently exist in Switzerland.

Although a large amount of literature on mine drainage exists, there is a rather poor knowledge about the long-term (i.e., decades to

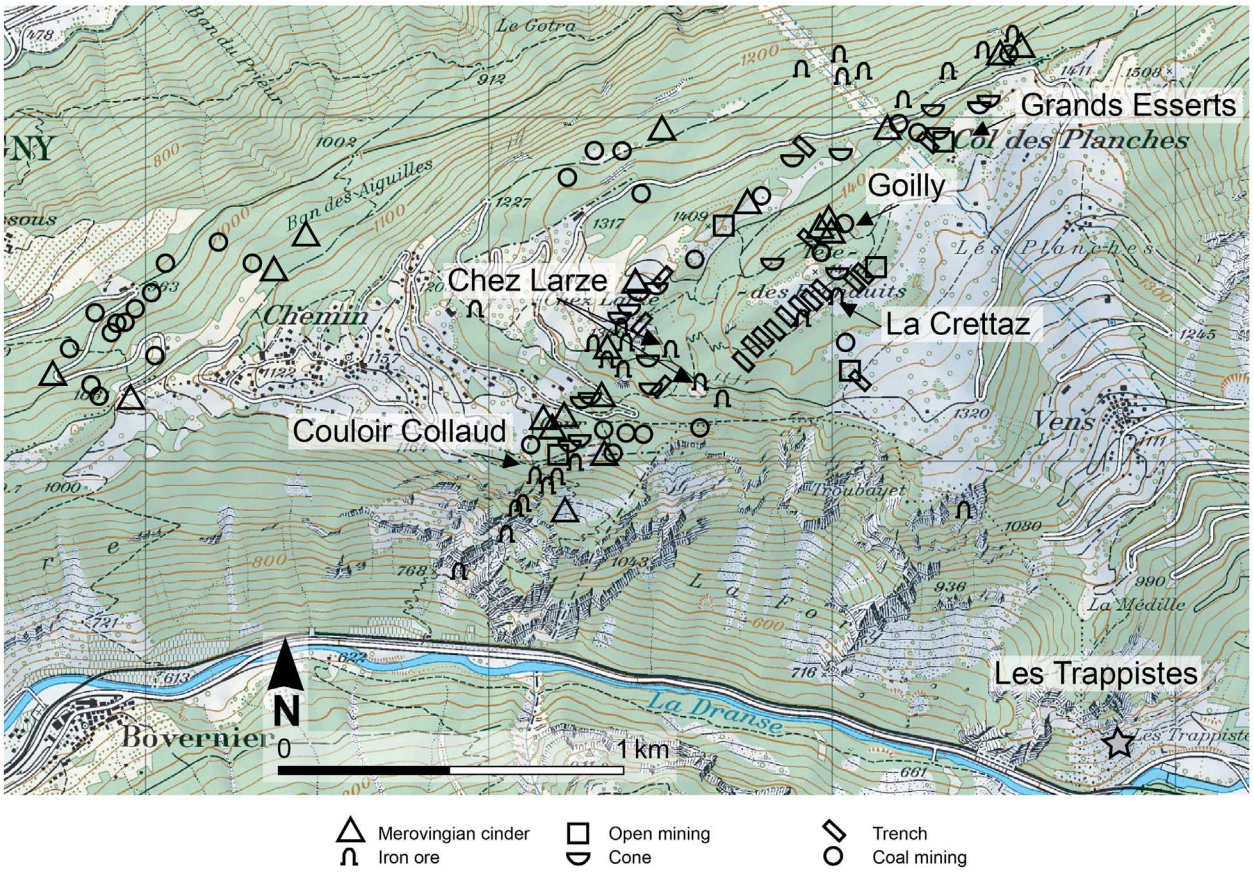

Fig. 2. Mining activities in the Mt. Chemin area (Ansermet, 2001). Reproduced by permission of swisstopo (BA17094).

centuries) behaviour of mine tailings with respect to the leaching of potentially toxic elements. Plante et al. (2011) performed laboratory tests to predict the geochemical behaviour of Ni with time in waste rock with low acid-generating potential. They came to the conclusion that Ni dissolution tends to increase with continued weathering if no preventive or control measures are undertaken at the site. A contrary effect was detected by Kim and Hyun (2015), who also tested leaching effects in laboratory experiments in which the solubility of most metals decreased with time and increasing seepage. Coulthard and Macklin (2003) used a modelling approach and revealed the exceptional longevity of contamination in fluvial systems.

Due to the limited explanatory power of laboratory tests with respect to the long-term behaviour, we attempted to determine if metal leaching can be traced using a relatively simple empirical approach. If feasible, this approach should then be used to extrapolate the results to other small mining sites in the Swiss Alps where similar minerals and elements were exploited. With increasing time, transformation reactions such as oxidation of sulphides, dissolution of trace metals and transfer of elements and pollutants from the solid to the liquid phase should diminish. Consequently, the subsequent transport to other components of the ecosystem, such as groundwater and vegetation, should also be reduced. We define the leaching rate of (trace) elements and pollutants as reactivity of a mining site. We assume that former mining sites and their corresponding mine tailings and waste become less reactive with increasing time, because the amount of problematic compounds diminish and/or easily weatherable minerals are transformed into more stable ones with the accompanying effect that elemental leaching is reduced. We hypothesised that such long-term changes are discernible by using a chronosequence approach. Chronosequences usually help to measure trends and rates of chemical weathering and transformation (see Dahms et al., 2012). The time over which natural chemical weathering occurs (White and Hochella, 1992) can usually not be reproduced by experimental studies (Dahms et al., 2012; White and Brantley, 2003). Chronosequences are thus very useful for estimating field weathering rates. Our aim was to find sites that were exploited at different time periods to derive a chronosequence. Using a chronosequence approach we then tried to measure the reactivity of individual sites. Based on this, we developed a concept to very roughly estimate this reactivity over a larger area using the surface age of soils that formed on such mine tailings.

2. Investigation area

Due to the already existing datasets and information about former mining activities, Mont Chemin, located near Martigny (canton of Valais, Switzerland), was selected as a case study (Fig. 1).

The area of Mont Chemin is mostly at an altitude of approximately 1100–1450 m a.s.l. (with 'Tête des Econduits' as the highest elevation). Annual precipitation is approximately 1000–1200 mm per year (BAFU, 2007). The Mont Blanc massive dominates the geology with its gneiss and crystalline schists, which occur on the southern and northern slopes of Mont Chemin (Fig. 1). Of particular importance is the intrusion of dykes coupled with hydrothermal veins at the 'Tête des Econduits'. These dykes contain a considerable amount of fluorite, galena (with additions of silver) and Fe-ore (Fe-oxides such as magnetite) that were the basis of the mining activities at Mont Chemin (Ansermet, 2001). In addition, palaeorhyolite dykes and some marble can partially be found.

Table 1
Overview of mining activities in the investigation area, soil profiles and surface ages.

Mining period	Name of the mine	Explored metals	Soil profile-nr and designation	Last mining activities [CE]	Soil age [a]	Dating source	Coordinates of soil sites [°North/°East]	Altitude [m a.s.l.]
Merovingian epoch 556–669 CE and Early Middle Ages 500–1050 CE	Goilly	Fe-ore (hematite)	Profile 3 Goilly	976–1017	1018	^{14}C-method	46.0932/7.1155	1451
Middle Ages until 16th century	Peiloz, Val de Bagnes	Pb and Ag (galena)	Profile 10 Peiloz-1 (Val de Bagnes)	1549	465	Guénette-Beck et al. (2009)	46.0524/7.2114	1617
			Profile 11 Peiloz-2 (Val de Bagnes)	1723	291	Guénette-Beck et al. (2009)	46.0518/7.2109	1630
Industrial revolution (1800–1875)	Grands Esserts	Fe-ore (magnetite)	Profile 8 Grands Esserts	1800	214	Ansermet (2001)	46.0945/7.1198	1433
	Les Trappistes	Pb and Ag (galena)						
	La Crettaz	Pb and Ag (galena)	Profile 7 La Crettaz-2	1864	150	Ansermet (2001)	46.0910/7.1150	1419
	Chez Larze I und III	Fe-ore (magnetite)	Profile 6 Chez Larze I	1873	141	Hugi et al. (1948)	46.0903/7.1074	1335
			Profile 1 Chez Larze III-1	1850	164	Ansermet (2001)	46.0899/7.1084	1335
			Profile 2 Chez Larze III-2	1850	164	Ansermet (2001)	46.0898/7.1085	1332
20th century	Couloir Collaud III	Fe-ore (magnetite)	Profile 5 Couloir Collaud III	1925	89	Hugi et al. (1948)	46.0858/7.1045	1078
	Les Trappistes	Fluorite	Profile 9 Les Trappistes	1946	68	Ansermet (2001)	46.0796/7.1273	699
	La Crettaz	Fluorite	Profile 4 La Crettaz-1	1976	38	Ansermet (2001)	46.0911/7.1148	1425

At undisturbed sites (not affected by mining activities), Dystric Cambisol is dominant (WRB: IUSS Working Group, 2014). According to the Soil Taxonomy (Soil Survey Staff, 2014), the soil moisture regime is udic (humid conditions, < 90 days/year with dry soil) at all sites, and the soil temperature regime is cryic (mean annual temperature < 8 °C, no permafrost). Maximum precipitation occurs during the summer and autumn months.

In addition to Mont Chemin, two sites (former Ag-mines) with similar geological composition (gneiss) in an adjacent valley (southeast of Mont Chemin; Val de Bagnes; Fig. 1) were included. From a historical and archaeological point of view, all of these sites are well documented (Ansermet, 2001; Guénette-Beck et al., 2009).

Since the Ancient World, and especially in the past two centuries, metal ores were mined on Mont Chemin (Fig. 2, Table 1). Some minor last metal ore mining activities occurred in 1943 (Ansermet, 2001). Mining took place in galleries and near-surface sites. Some of the smelting occurred on site. The main ores that were mined were magnetite and galena (Ansermet, 2001; Egli et al., 2011a). Furthermore, marble and fluorine-containing minerals were exploited. The mine tailings were dumped on site. With time, young and shallow soils have developed on the tailings. In total, 11 sites were investigated covering a time span of approximately 1000 years (Table 1).

3. Materials and method

3.1. Sampling procedure

In an earlier investigation (Egli et al., 2011b), the whole area was checked for metal contamination using an energy dispersive field-XRF (NITON XL3t XRF Analyzer). Such an XRF is particularly suited for trace metal detection. Surface soil samples were collected, homogenised (as far as possible) in plastic bags and then measured. This investigation provided a first glimpse of the spatial variability of trace metal contamination due to mining (Fig. 3). Based on these results and again using the field-XRF, 11 sites on the mine tailings were selected. These sites varied in their time span since the last exploitation and, thus, surface ages (for soil formation) are different giving rise to a chronosequence. At each site, a soil profile was dug down to the unweathered parent material (mine wastes). A total of 1–2 kg of soil material per horizon was taken for the analyses (Hitz et al., 2002). The bulk density was measured using a soil core sampler. In the oldest profile (Goilly), a small amount of charcoal was detected and sampled for radiocarbon dating.

3.2. Chemical analyses

Oven-dried samples (70 °C) were sieved to < 2 mm (fine earth) and homogenised. Soil-pH (0.01 M $CaCl_2$) was determined using a soil:solution ratio of 1:2.5. Organic C and N contents (determined in duplicate) of the soil were measured at 550 °C using a C/H/N analyser (Leco). The standard reference material is EDTA (Säntis Analytical, article no SA502092) with C = 41.09%, H = 5.52%, N = 9.58%, and O = 43.8% (measured values were C: 41.11 ± 0.08%; H: 5.53 ± 0.08%; N: 9.57 ± 0.08%, and O: 43.79 ± 0.08).

Fe, Al and Mn concentrations were measured (in duplicate) after treatment with NH_4-oxalate (buffered at pH 3; McKeague et al., 1971) to determine both the weakly- and poorly crystalline phases and some of the organic phases (Mizota and van Reeuwijk, 1989). Total oxyhydroxide concentrations of Fe and Al were determined after treatment (in duplicate) of the soil with sodium-dithionite (McKeague et al., 1971). The dithionite-extraction predominantly separates amorphous, crystalline and organically bound Al- and Fe-oxyhydroxides from the soil (Borggaard, 1988). The extracts were centrifuged for 8 min at 4000 rpm and filtered (mesh size 0.45 μm, S & S, filter type 030/20). Element concentrations were measured using atomic absorption spectroscopy (AAnalyst 700, Perkin Elmer). Element concentrations were

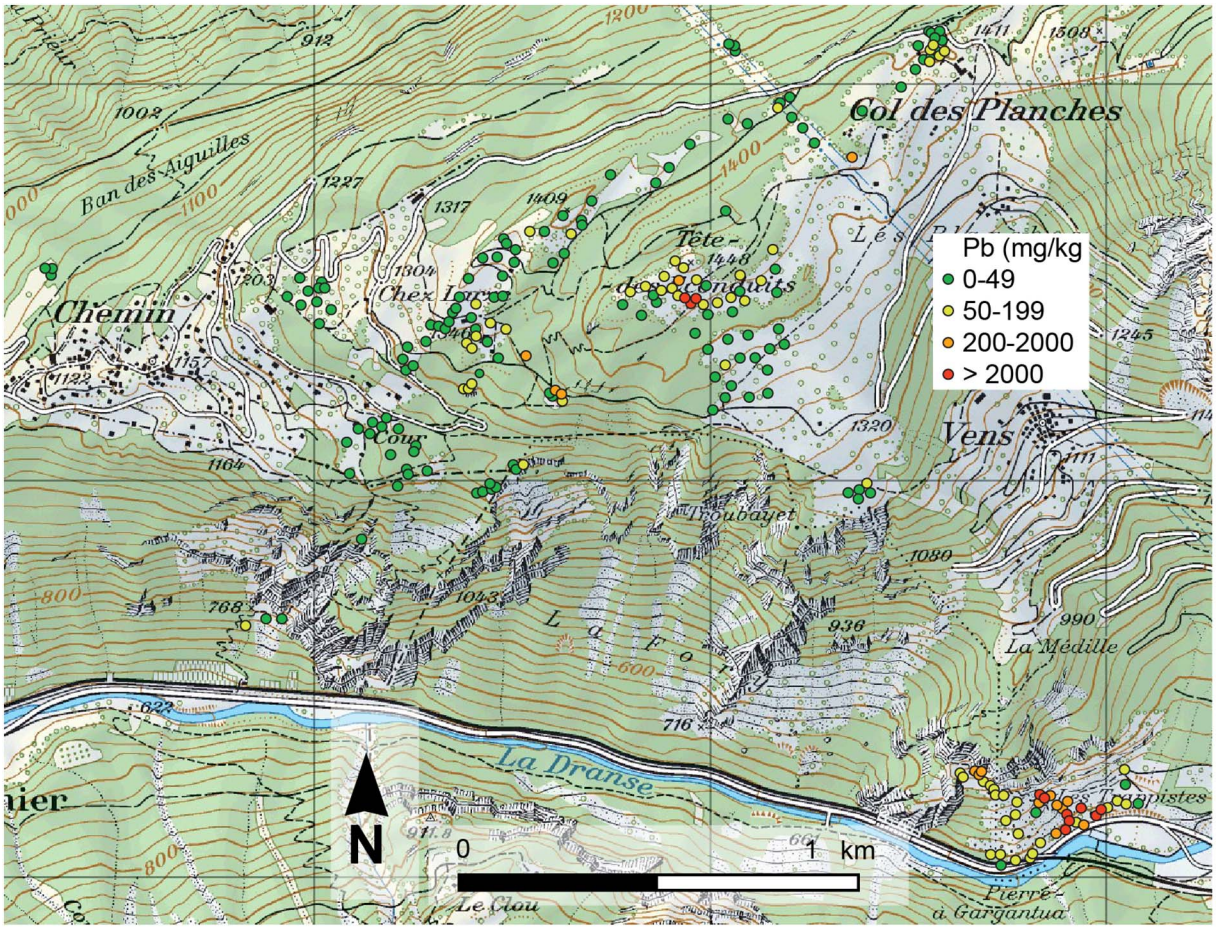

Fig. 3. Pb-concentrations in the topsoils measured by means of field-XRF. Reproduced by permission of swisstopo (BA17094).

furthermore controlled using standard addition (recovery ≥ 95%).

The total elemental content was determined by X-ray fluorescence. Soil material was milled to < 63 μm in a tungsten carbide disc swing mill (Fritsch Pulverisette). Powder samples (in duplicates) of approximately 5 g material were analysed with an energy dispersive He-flushed X-ray fluorescence spectrometer (ED-XRF, SPECTRO X-LAB 2000, SPECTRO Analytical Instruments, Germany). The quality of the analyses was checked using a soil reference material (Reference Soil Sample CCRMP SO-4, Canada Centre for Mineral and Energy Technology) with certified total element concentrations.

3.3. Soil mineralogy

We used XRD (X-ray diffraction) to analyse the soil mineralogical properties. An overview of the mineral content in the fine earth fraction (< 2 mm) was obtained by scanning milled and randomly oriented samples from 2 to 80°2θ with steps of 0.02°2θ at 10-s intervals using a Bruker AXS D8 Advance (CuKα). Data evaluation was conducted using DIFFRACplus EVA.

3.4. Radiocarbon dating of charcoal

The charcoal sample was cleaned using an acid-alkali-acid (AAA) treatment. The cleaned charcoal was then heated in quartz tubes under a vacuum with CuO (oxygen source) to remove any absorbed CO_2 in the CuO. The tube was then evacuated again, sealed and heated in the oven at 900 °C to obtain CO_2. The CO_2 of the combusted sample was mixed with H_2 (1:2.5) and catalytically reduced over iron powder at 535 °C to elemental carbon (graphite). After reduction, the mixture was pressed into a target, and carbon ratios were measured by Accelerator Mass Spectrometry (AMS) using a 0.2 MV radiocarbon dating facility (MICADAS) of Ion Beam Physics at the Swiss Federal Institute of Technology Zurich (ETHZ).

The calendar ages were obtained using the OxCal 4.2 calibration program (Bronk Ramsey, 2001, 2009) based on the IntCal 13 calibration curve (Reimer et al., 2013). Calibrated ages are given in the 1σ and 2σ range (minimum and maximum value for each).

3.5. Weathering indexes

Several indexes have been defined to characterise chemical weathering in soils. The general principle of all these indexes is similar and based on the ratio of 'mobile' cations (e.g., Ca, Mg, K, and Na) to an immobile element (Al and/or Si; or others such as Ti, Zr, Hf etc.). We used 'index B' of Kronberg and Nesbitt (1981) to characterise the general weathering trends. Index B is defined by the molar ratio of

Table 2
Some physical and chemical characteristics of the investigated soils (n.d. = not determined). The sites are listed in a chronological order (increasing age since last mining activities).

Profile	Soil horizon	Depth [cm]	Munsell colour	Bulk density [g/cm^3]	Rock fragments [%]	pH ($CaCl_2$)	C_{org} [g/kg]	N [g/kg]	C/N
Profile 4	A	0–10	2.5Y 4/3	1.00	51	5.3	28.2	4.18	6.7
La Crettaz-1	C1	10–30	2.5Y 5/2	1.72	62	5.8	2.4	3.44	0.7
	C2	30–60	2.5Y 5/2	1.60	68	5.95	2.9	3.19	0.9
Profile 9	A1	0–16	2.5Y 4/2	1.21	56	7.35	4.5	3.03	1.5
Les Trappistes	A2	16–30	5Y 4/2	1.42	67	7.3	2.3	3.36	0.7
	AC	30–60	5Y 5/2	1.35	75	7.55	2.5	3.84	0.7
Profile 5	CA	0–3	10YR 2/2	1.27	49	7.1	42	5.61	7.5
Couloir Collaud III	AC	3–13	10YR 3/2	1.55	74	7.25	32.3	3.03	10.6
	C	13–43	n.d.	n.d.	n.d.	n.d.	n.d.	n.d.	n.d.
Profile 6	A1	0–8	10YR 3/2	1.05	36	4.85	32.3	5.46	5.9
Chez Larze I	A2	8–16	10YR 3/2	1.49	68	6.1	7.7	3.55	2.2
	(B)C	16–31	n.d.	n.d.	n.d.	n.d.	n.d.	n.d.	n.d.
Profile 7	C1	0–15	10YR 5/2	1.20	75	4.3	56.1	5.17	10.9
La Crettaz-2	C2	15–40	10YR 5/2	1.32	75	4.2	46.4	4.72	9.8
Profile 1	BC	0–10	10YR 4/3	1.32	39	4.8	23.2	4.85	4.8
Chez Larze III-1	BAb	10–40	10YR 4/2	1.27	52	4.9	10.7	4.51	2.4
	Bb	40–58	10YR 4/3	1.06	31	5.1	6.7	3.11	2.2
	BCb	> 58	10YR 5/4	1.40	50	5.1	3.2	3.36	0.9
Profile 2	A1	0–10	10YR 2/1	1.08	67	6.05	61.4	1.69	36.4
Chez Larze III-2	A2	10–20	2.5Y 3/2	1.34	72	6.7	31.7	4.19	7.6
	A3	20–40	2.5Y 3/2	1.29	65	6.9	8.8	3.65	2.4
	C	40–60	2.5Y 4/1	1.57	69	6.9	5	4.07	1.2
Profile 8	A	0–12	10YR 3/2	1.30	58	6.2	16.3	3.77	4.3
Grands Esserts	CB	12–16	10YR 4/3	1.25	49	7.05	4.6	3.58	1.3
	C	16–31	10YR 5/3	1.29	74	7.1	2.7	3.46	0.8
Profile 11	A	0–12	2.5Y 4/4	1.34	68	5.9	2.5	3.26	0.8
Peiloz-2	BC1	12–35	2.5Y 4/3	1.35	68	6.1	2.8	3.35	0.8
	BC2	35–42	2.5Y4/3	1.45	75	6.1	< 2.0	3.39	n.d.
Profile 10	A	0–5	5 YR 4/6	1.09	39	3.8	11.3	3.91	2.9
Peiloz-1	AB	5–30	10YR 3/4	1.43	72	5.6	< 2.0	2.97	n.d.
	C	30–40	5Y 5/2	1.41	49	5.65	< 2.0	3.53	n.d.
	Ab	40–42	10YR 4/6	n.d.	n.d.	n.d.	n.d.	n.d.	n.d.
	ABb	42–53	2.5Y 4/4	1.2	52	5.4	2.1	3.47	0.6
	BCb	53–80	2.5Y 3/3	1.34	65	5.8	< 2.0	2.95	n.d.
Profile 3	A	0–8	10YR 3/2	1.00	66	4.8	66.8	6.34	10.5
Goilly	B	8–28	10YR 5/3	1.27	61	4.6	15.9	3.9	4.1
	BC	28–50	10YR 5/3	1.60	58	4.3	6.2	3.93	1.6
	BAb	50–56	10YR 5/3	1.34	55	4.1	13.2	3.8	3.5

$$B = \frac{CaO + K_2O + Na_2O}{Al_2O_3 + CaO + K_2O + Na_2O} \quad (3)$$

The index B refers to silicate weathering. Consequently, the Ca content (to account for dolomite and calcite) was corrected. To estimate the mobility of trace metals, the ratio to immobile elements (Ti, Zr, V and Hf) was performed according to

$$R_i = \frac{C_i}{C_j} \quad (4)$$

where R_i is the corresponding ratio of element i, C_i is the concentration of element i and C_j the concentration of the considered immobile element j.

3.6. SEM-EDS

The soil samples were impregnated with the resin Viscovoss N50S and hardener MEKP505F at the Laboratory of Soil Science and Geoecology, University of Tübingen. Then, the impregnated blocks were cut and ground to 100 μm. The thin sections were polished and analysed by scanning electron microscopy (Jeol 6390LA) at the Institute of Geochemistry and Petrology (ETH, Zurich), using energy-dispersive X-ray spectroscopy (SEM-EDX) using a solid state EDS detector combined with the Thermo scientific software NSS3 under high vacuum conditions. An acceleration voltage of 15 kV was employed for all analyses and phases were analysed in a standard-less mode. In addition, BSE images were recorded.

3.7. Database analysis of the Swiss Geotechnical Commission (Schweizerische Geotechnische Kommission)

The Swiss Geotechnical Commission (SGTK) has the mandate (given by the federal government) to investigate usable mineral resources in Switzerland, archive samples and data, and make this information accessible to interested parties. For this purpose, the SGTK maintains a mining database (historic) with information about the sites (coordinates), mining activities over time, primary and secondary minerals mined (and related chemical elements), amount of exploited rocks and minerals, etc. One aim of this work was now to find sites in Switzerland with moderately comparable conditions to Mont Chemin. As a consequence a search was performed for sites with acidic conditions, i.e., sites with silicate parent rocks (gneiss, granite, mica-schists). Sites with calcareous rocks were excluded because carbonates counteract acidification and strongly limit the mobility of most trace metals. Furthermore, a focus was given to the last mining activities to derive a

Table 3
Total pedogenetic Fe, Al and Mn phases (dithiontite extractable phases (d)), weakly and poorly crystalline phases (oxalate extractable phases (o)) and crystallline pedogenetic phases (d)-(o). The sites are listed in a chronological order (increasing age since last mining activities).

Profile	Soil horizon	Depth [cm]	Mn(o) [g/kg]	Fe(o) [g/kg]	Al(o) [g/kg]	Fe(d) [g/kg]	Al(d) [g/kg]	Fe(d)-Fe(o) [g/kg]	Al(d)-Al(o) [g/kg]
Profile 4	A	0–10	0.75	0.93	0.77	19	5.44	17.6	4.68
La Crettaz-1	C1	10–30	0.56	1.03	0.71	19	6.93	17.8	6.22
	C2	30–60	0.73	0.96	0.39	22	7.55	21.1	7.16
Profile 9	A1	0–16	0.88	1.88	0.61	84	3.19	81.7	2.58
Les Trappistes	A2	16–30	0.8	1.65	0.54	77	3.04	75.8	2.5
	AC	30–60	0.62	2.07	1.04	85	5.84	82.9	4.81
Profile 5	CA	0–3	0.51	2	0.5	114	7.88	111.7	7.38
Couloir Collaud III	AC	3–13	0.56	2.99	0.68	121	9.02	118	8.33
	C	13–43	0.11	4.4	0.32	35	3.75	30.1	3.43
Profile 6	A1	0–8	1.03	11.42	1.18	288	17.14	276.5	15.96
Chez Larze I	A2	8–16	3.23	6.67	1.37	373	19.87	366.3	18.49
	(B)C	16–31	0.7	4.9	0.35	126	4.96	121.4	4.61
Profile 7	C1	0–15	0.54	2.5	0.54	48	7.6	45.6	7.06
La Crettaz-2	C2	15–40	0.47	2.7	0.36	39	5.67	36.2	5.31
Profile 1	BC	0–10	1.29	6.79	0.51	349	8.89	342.5	8.37
Chez Larze III-1	BAb	10–40	1.23	5.53	0.94	335	17.12	329.7	16.18
	Bb	40–58	0.45	3.64	1.07	166	12.15	162.7	11.07
	BCb	> 58	0.28	3.34	0.99	155	12.71	151.8	11.72
Profile 2	A1	0–10	1.02	3.74	0.91	177	9.31	173.3	8.4
Chez Larze III-2	A2	10–20	1.02	2.54	0.54	173	6.11	170.9	5.57
	A3	20–40	1.09	1.72	0.59	186	6.98	184.2	6.38
	C	40–60	1.31	2.33	0.59	232	7.22	229.6	6.62
Profile 8	A	0–12	1.19	10.63	1.28	345	12.07	334.1	10.8
Grands Esserts	CB	12–16	1.03	3.28	0.57	149	8.71	145.7	8.14
	C	16–31	0.85	2.02	0.42	113	5.51	110.6	5.1
Profile 11	A	0–12	6.93	32.61	1.32	276	7.35	243.2	6.03
Peiloz-2	BC1	12–35	6.34	17.32	1.1	193	5.72	176.1	4.62
	BC2	35–42	6.45	14.01	1.06	229	5.43	214.6	4.37
Profile 10	A	0–5	0.14	12.37	0.51	792	9.63	779.4	9.12
Peiloz-1	AB	5–30	1.03	5.93	1.89	298	8.76	292.1	6.88
	C	30–40	0.45	0.48	1.08	12	3.75	12	2.67
	Ab	40–42	n.d.	n.d.	n.d.	n.d.	n.d.	n.d.	n.d.
	ABb	42–53	6.93	32.61	0.92	116	8.03	83	7.11
	BCb	53–80	10.03	21.75	1.33	119	5.34	97.4	4.01
Profile 3	A	0–8	1.36	1.31	0.47	120	7.87	118.9	7.4
Goilly	B	8–28	1.27	1.35	0.84	111	8.54	109.4	7.7
	BC	28–50	0.67	1.4	0.91	80	7.75	78.8	6.84
	BAb	50–56	0.47	2.83	1.31	113	12.46	109.9	11.14

n.d. = not determined.

time specification that can be linked to a specific weathering behaviour. In addition, a specific search was conducted for Pb and Cu to compare with the conditions at Mont Chemin.

A geographic information system (GIS) was used for evaluating and displaying spatial data from the study area and Switzerland. All spatial data were processed using Environmental Systems Research Institute (ESRI) ArcCatalog and ArcMap software, v10.2.2, with ArcInfo license. Basic data were available through the Swiss federal geoportal (www.geo.admin.ch).

3.8. Statistics and trend analyses

A correlation and multiple linear regression were carried out to help explaining the behaviour of trace metals in the soil and describe them as a function of controlling factors. As the data did not always show a normal distribution (Shapiro-Wilk test), correlation and multiple regression (where a normal distribution is required) analyses were performed after a log-transformation of the data. All analyses were checked by a two-sided test for significance. In addition, the multiple linear regression analysis was performed using standardised regression coefficients.

The chronofunction of elemental loss was fitted to data using non-linear regression procedures. A best fit of the time trends was obtained by using the following two models (sigmoid functions):

The first sigmoid function (model 1) is described by an exponential decay model (cf. Lichter, 1998):

$$f(t) = a + (b - a)e^{-kt} \quad (5)$$

where a represents an asymptote, b the initial quantity, and k the decay constant. The second (model 2) is given by (Lichter, 1998):

$$f(t) = \frac{a}{(1 + e^{b(t-e)})} + d \quad (6)$$

where a = range of the wood property, t = time, b = slope coefficient, c = time (in years) of the maximal rate of change and d = asymptotic value (t = ∞).

4. Results

4.1. General soil properties, metal contamination and minerals

Most of the soils were of an A-C horizon sequence that is typical for weakly developed soil profiles. Not surprisingly, the soils exhibit high rock fragment content (Table 2). Consequently, water permeability is high, and no water stagnation could be detected. All investigated soils

Table 4
Concentrations of selected metals in the soils (fine earth; measured with XRF in the laboratory). The sites are listed in a chronological order (increasing age since last mining activities).

Profile	Soil horizon	Depth [cm]	Cr [mg/kg]	Mn [g/kg]	Fe [g/kg]	Co [mg/kg]	Ni [mg/kg]	Cu [mg/kg]	Zn [mg/kg]	As [mg/kg]	Cd [mg/kg]	Pb [mg/kg]	U [mg/kg]
Profile 4	A	0–10	48.0	1.07	7.3	3.0	0.5	199	2869	0.4	8.8	22,720	0.4
La Crettaz-1	C1	10–30	54.4	0.71	7.8	3.0	0.5	203	2939	35.6	7.2	22,160	0.4
	C2	30–60	64.8	1.03	8.8	3.0	0.5	248	3177	26.2	7.9	22,760	0.4
Profile 9	A1	0–16	63.4	1.72	38.9	53.2	24	131	3914	8.9	16.7	4869	2.5
Les Trappistes	A2	16–30	67.7	1.79	42.4	55.5	24.8	135	4630	0.1	19.3	5196	3.2
	AC	30–60	93.4	1.61	46	42.4	38.4	145	4384	42.9	21.5	3810	1.1
Profile 5	CA	0–3	53.6	3.06	136.4	28.2	29.4	76	553	34.1	4.7	48	0.4
Couloir Collaud III	AC	3–13	43.3	3.38	132.8	28.2	23.9	90	535	28.9	4.2	65	0.4
Profile 6	A1	0–8	67.5	2.43	135.2	138.2	26.4	46	287	233.2	1.2	85	0.4
Chez Larze I	A2	8–16	61.7	7.94	246.2	361	25.1	82	278	763.7	1.3	81	0.4
Profile 7	C1	0–15	69.7	0.77	19.3	16.7	23.9	63	457	5.1	3	6239	2.0
La Crettaz-2	C2	15–40	78.4	0.79	18.6	14.5	22.2	47	293	0.6	2.8	5558	1.3
Profile 1	BC	0–10	53.2	3.79	212.6	3.0	16.4	1524	377	84.1	2.1	104	0.4
Chez Larze III-1	BAb	10–40	74.3	2.81	158.3	3.0	22.8	1419	261	75.2	1.7	68	0.4
	Bb	40–58	78.6	1.82	126.4	16.2	33.7	352	255	38.2	1.8	53	1.4
	BCb	> 58	75.9	1.93	153.4	3.0	30.7	407	270	32.4	2.2	63	6.8
Profile 2	A1	0–10	32.2	3.65	116.9	14.2	18.1	333	810	39.9	5.4	295	0.4
Chez Larze III-2	A2	10–20	35.1	3.73	130.8	8.9	16.5	433	1052	29.4	5.9	330	0.4
	A3	20–40	66.8	4.05	153.1	16.2	30.1	744	931	23.2	5.7	352	0.4
	C	40–60	58.6	4.22	168	3.0	19.7	1252	1202	18.4	7.3	670	0.4
Profile 8	A	0–12	26.3	2.03	281.8	24.8	18.9	7722	556	154.5	1.4	353	0.4
Grands Esserts	CB	12–16	88.6	1.59	60.3	26.9	54.1	605	112	67.1	0.8	52	1.1
	C	16–31	54.7	1.42	60.4	33.3	31.8	662	108	55.7	1.2	52	0.4
Profile 11	A	0–12	95.3	1.97	52.4	103.5	32.1	144	25,210	575.4	20.9	8461	5.0
Peiloz-2	BC1	12–35	101.1	1.89	53.7	90.7	32.7	148	25,410	583.7	22.2	9521	5.1
	BC2	35–42	107.5	1.79	72.8	70.5	57.8	128	22,860	12.4	19.8	6298	0.5
Profile 10	A	0–5	58.1	0.26	105.7	3.0	0.5	172	9100	34.3	23.5	74,960	8.3
Peiloz-1	AB	5–30	83.1	1.86	62.8	21.0	27.5	308	14,450	54.4	12.6	18,780	11.5
	C	30–40	93.4	0.74	44.9	67.7	35.7	36	5894	2.4	8.6	1380	0.9
	ABb	42–53	62.9	1.08	39.7	56.0	23	41	6671	21.4	6.5	2412	1.8
	BCb	53–80	92.8	1.73	52.2	66.5	43.8	88	10,900	54.3	15.2	2607	2.0
Profile 3	A	0–8	40.3	1.88	29.5	22.9	12.7	66	77	106.4	0.7	37	0.4
Goilly	B	8–28	41.9	1.63	30.9	23.7	14.8	87	61	112.5	0.8	25	0.4
	BC	28–50	67.7	0.89	36.7	18.7	13.3	55	59	71.0	0.6	25	0.4
	BAb	50–56	77.2	0.85	40.1	26.0	22.2	50	80	68.1	0.4	36	1.1

Table 5
Radiocarbon ages of the dated charcoal.

UZH number	Site and horizon	Depth [cm]	^{14}C age (uncal.)	δ^{13}C	Calibrated age
6269	Profile 3 Goilly BAb	50–56	1060 ± 25 BP	− 26.6 ± 1.0‰	976–1017 cal CE (1σ-range)

can be classified as Technosols. In most cases, organic carbon decreased with increasing soil depth. Some profiles (e.g., profile 3 in Goilly) show a 'polygenetic' structure with the buried soil horizons. The soil colours that were in the range of 5Y to 10YR also indicate the young and weakly developed character of the soils (Harden, 1982). The pH-values range from neutral to acidic (Table 2). All of the sites were characterised by high to very high Fe-contents with a large proportion of crystalline forms (with a range of 71.6–100% and median value of 97.8%; Table 3). This is not surprising as most of the sites were also exploited for Fe-ore (cf. Table 1). Organic carbon ranged from very low up to values that are typical for forest soils. In general, the org. C/N ratios (Table 2) strongly decreased with increasing soil depth and exhibited in the subsoils particularly low values in some cases.

Profiles 1 and 2 (Chez Larze III-1 and III-2) were in close vicinity to a mining cave and were characterised by high Cu (330–1520 mg/kg), Zn (380–1200 mg/kg), Pb (50–670 mg/kg) and As (84 mg/kg) contents (Table 4). A real 'humus' layer was absent in profile 1. Soil profile 3 was the most developed and weathered. Here, a weak B horizon was morphologically discernible. Soil evolution tends towards Cambisol. At this site, the As content was elevated (up to 113 mg/kg). In this profile, charcoal fragments were found and could be radiocarbon-dated. The charcoal gave indications as to when this site was mined for the last time. In the surrounding of this area, small pieces of scoria were found. Smelter processing obviously occurred in this location. The calibrated age of the charcoal was approximately 1000 years BP (Table 5). Profiles 4 (La Crettaz-1) and 5 are both young sites. Consequently, only a very shallow soil with some organic matter in the surface horizon was developed. In profile 4, pieces of galena were found, giving rise to very high Pb contents of up to 22 g/kg (Table 4). Profile 6 was already slightly more developed and exhibited a clear A horizon. Additionally, in profile 7 (La Crettaz-2), very high Pb concentrations were measured (5.5–6.2 g/kg). Profile 8 (Grands Esserts) exhibited high Cu (up to

Table 6
Approximate mineral composition of selected profiles and soil horizons. The sites are listed in a chronological order (increasing age since last mining activities).

Site	Soil horizon	Qz	Cc + Dol	Alb	Or	Mica + Verm + Chlo	Fluorite	Cu-minerals[a]	Pb-minerals[b]	Zn-minerals[c]	Fe-minerals		
											Goethite	Hem, Mag	Pyr, Chalpyr
		[%]											
Profile 4	A	36	0	3	0	1	56	0	3	0	0	1	0
La Crettaz-1	Skeleton	72	1	1	0	1	24	0	1	0	0	0	0
Profile 9	A1	54	6	2	0	4	33	1	1	1	0	0	1
Les Trappistes	AC	85	0	2	2	4	0	2	1	2	0	3	2
Profile 5	CA	65	6	4	0	8	1	0	0	0	1	10	1
Couloir Collaud III	C	49	6	6	0	7	1	10	0	0	0	13	10
Profile 6	A1	79	0	7	0	6	0	0	0	0	1	7	0
Chez Larze I	(B)C	0	0	0	0	0	0	0	0	0	0	0	0
Profile 7	C1	66	1	1	1	0	30	0	1	0	0	0	0
La Crettaz-2	C2	64	1	1	0	0	34	0	1	0	0	0	0
Profile 1	BAb	79	0	4	0	5	1	0	0	0	1	5	0
Chez Larze III-1	BCb	69	0	4	0	7	1	0	0	0	0	16	0
Profile 2	A1	60	0	6	0	10	5	0	0	0	1	9	0
Chez Larze III-2	C	66	8	5	0	11	1	0	0	0	0	7	0
Profile 8	Ah	59	1	2	0	9	0	0	0	0	1	25	2
Grands Esserts	C	81	6	4	2	3	0	0	0	0	0	2	1
Profile 3	A	93	2	1	1	1	0	0	0	0	1	2	0
Goilly	BC	89	2	2	1	2	0	0	0	0	1	2	0

Qz = quartz, Cc = calcite, Dol = dolomite, Alb = albite, Or = orthoclase, Mica = biotite + muscovite, Verm = vermiculite, Chlo = chlorite, Hem = hematite, Mag = magnetite, Pyr = pyrite, Chalpyr = chalcopyrite.
[a] Cu-minerals: malachite, azurite, chalcopyrite.
[b] Pb-minerals: galena, cerussite.
[c] Zn-minerals: sphalerite.

7.7 g/kg), Pb (up to 350 mg/kg) and As (up to 155 mg/kg) contents. Soil profile 9 was very young and consequently very weakly developed. Only a small amount of organic C accumulated thus far. Similar to profile 4, high concentrations of Zn (up to 4.6 g/kg) and Pb (up to 5.2 g/kg) were measured. Profiles 10 and 11 are close to the former mine Peiloz (Val de Bagnes). At both sites, very high Pb (up to 75 g/kg) and Zn (up to 25 g/kg) contents were detected.

A spatial overview of Pb in the topsoil (using field-XRF) is given in Fig. 3. Particularly high Pb values were measured at 'Tête des Econduits', 'Chez Larze', 'Col des Planches' and 'Les Trappistes'. Field-XRF measurements correlated well with laboratory XRF measurements (Egli et al., 2011a) but resulted in an underestimation of the real value by a factor of 1.5 for Pb.

An overview of the mineral composition in the fine earth is given in Table 6. Principally, the detected main minerals indicate a granitic composition. All sites have a high proportion of quartz, some feldspar, sheet silicates and, in several cases, a small amount of carbonates. In addition, Fe-minerals were abundant and at several sites, Fluorite was found. Although the Pb content is quite high at several sites, Pb- or Zn-minerals were detected only at some sites. This problem is likely related to the XRD itself, as it cannot detect minerals at the trace level.

4.2. Temporal trends

Over the considered time span, the acidity of the soil steadily increased (decreasing pH). At the start of weathering, most soils had

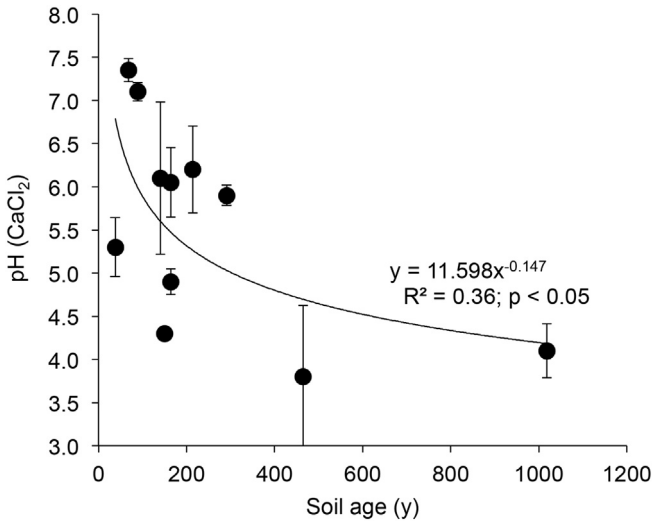

Fig. 4. Average (± SD) pH-values ($CaCl_2$) of the soil profiles at the investigated mining sites as a function of soil age (time since abandonment of mining activities).

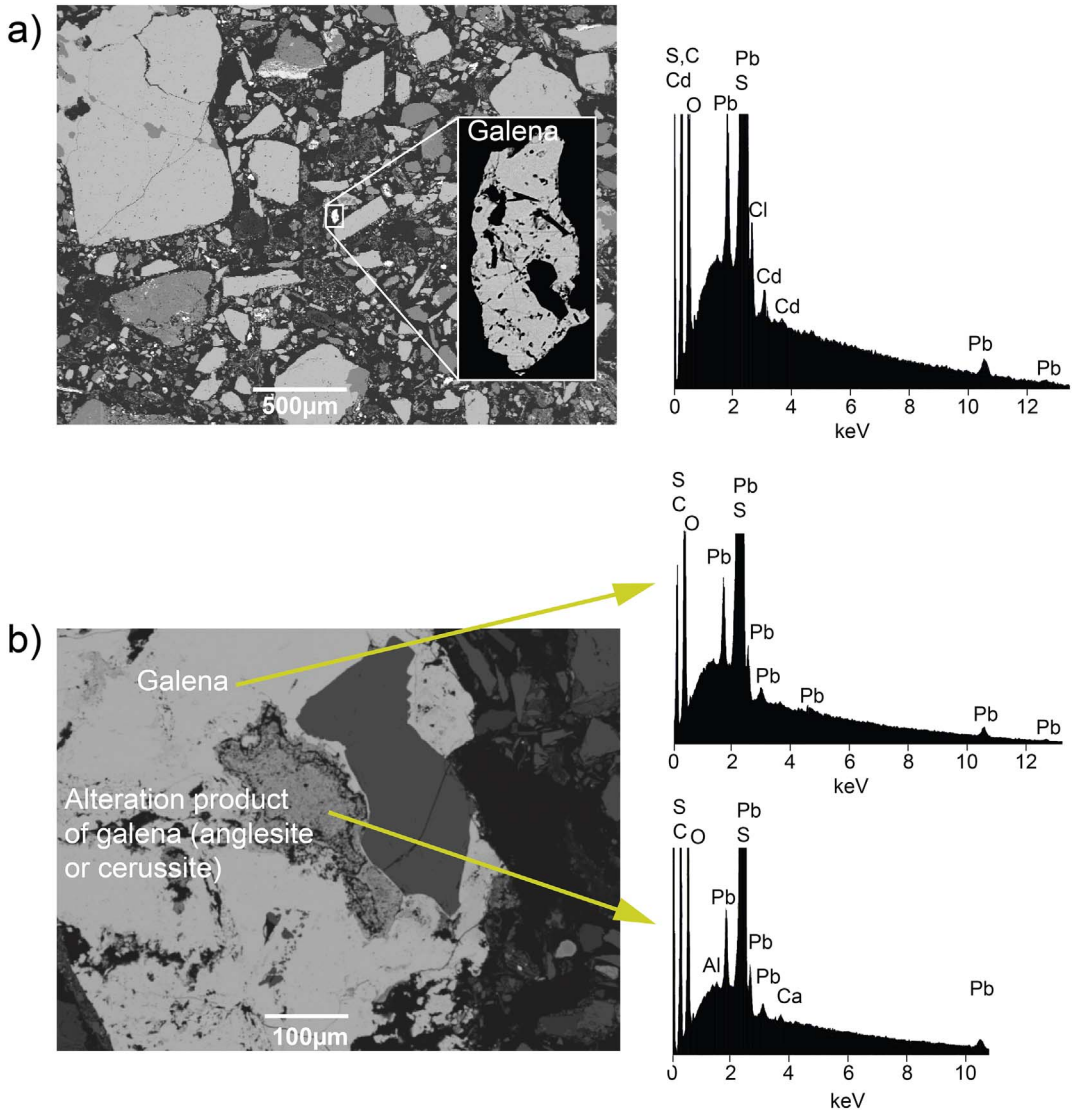

Fig. 5. SEM micrographs with EDS analyses of a) a pure galena and b) a weathered galena with alteration products (probably anglesite or cerussite) in the inner part (38 year-old site La Crettaz).

a pH in the neutral range (Fig. 4), but after a few centuries, the pH tended to approximately 4. Soil acidification is a natural process but also an anthropogenic process due to the exposure of sulphides to the atmosphere and subsequent oxidation of reduced compounds tending to form strong acids (H_2SO_4). Sulphide-minerals such as galena or Fe-sulphides react fast or even very fast and are either dissolved or transformed into new minerals. Galena may be transformed into anglesite, $PbSO_4$, or cerussite, $PbCO_3$, that are very common weathering products (Huff, 1976; Fig. 5). Cerussite and anglesite commonly occur either as in situ replacement of galena and/or as euhedral crystals in cavities of former, partially dissolved galena. During progressive weathering anglesite typically disappears first followed by cerussite (Keim and Markl, 2015).

The oxyhydroxides (poorly crystalline and crystalline forms) seem to increase with time, although the variability was considerable (Fig. 6). The crystalline forms were obtained by difference between the dithionite and oxalate extractable contents. The temporal trend was, however, only for Al(o) and Fe(d) significant. This suggests that with active weathering also new and fresh (poorly crystalline forms; or transformation of poorly crystalline forms into more crystalline) forms were produced over time. Similarly, the org. C and N stocks in the soils increased with time (data not shown; Table 2).

The weathering index B (Fig. 7) distinctly decreased with increasing mine tailing exposure time. Weathering of silicates obviously proceeded relatively fast over the observed time span. Base cation leaching seems to be particularly intensive during the first 200 years. Thereafter, the trend is much less pronounced, and the rate of change in base cation content is strongly reduced. Fine earth and rock fragments displayed almost identical behaviour (Fig. 7).

When comparing trace metals (Cd, Cr, Cu and Pb) with an immobile

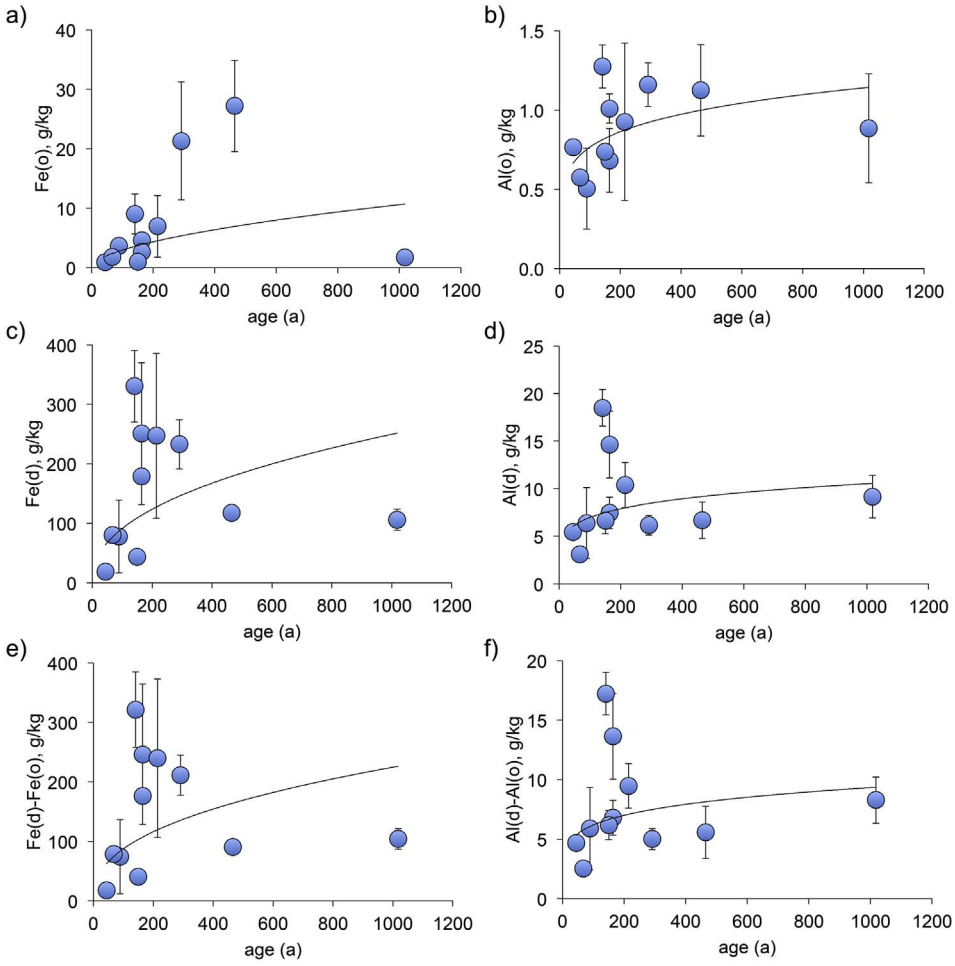

Fig. 6. Temporal evolution of the a) + b) oxalate (poorly crystalline phases) and c) + d) dithionite (sum of poorly and crystalline phases) extractable contents of Fe and Al (average values of the weathered profile; error bars represent ± SD). The crystalline phases (e + d) are obtained from the subtraction of the oxalate minus the dithionite extractable content.

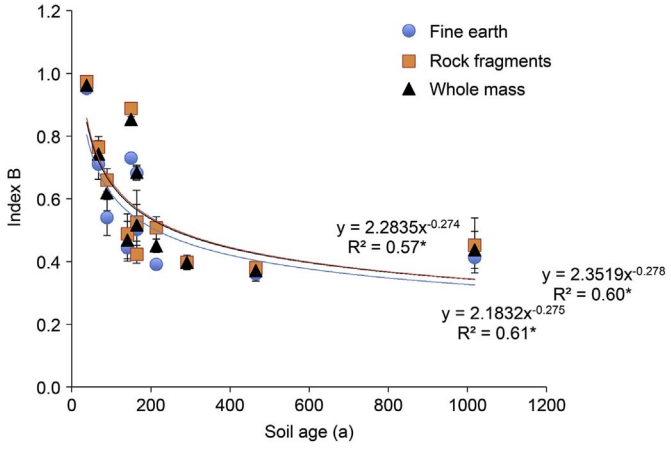

Fig. 7. Average index B values (± SD) of the soil profile (weathered part) of the sites as a function of time (soil age).

element (Hf; Fig. 8), a similar tendency can be detected. A distinct part of these metals seemed to be either leached completely or be transported to greater depths. The ratio of trace metals to Hf showed in most cases a clear and highly significant trend (with decreasing ratios) as a function of time (Fig. 8). In general, the rate of change was highest during the first 200 years of soil development. Between approximately 200–400 years, this rate was strongly reduced, tending to very small values for exposure ages of > 400 years.

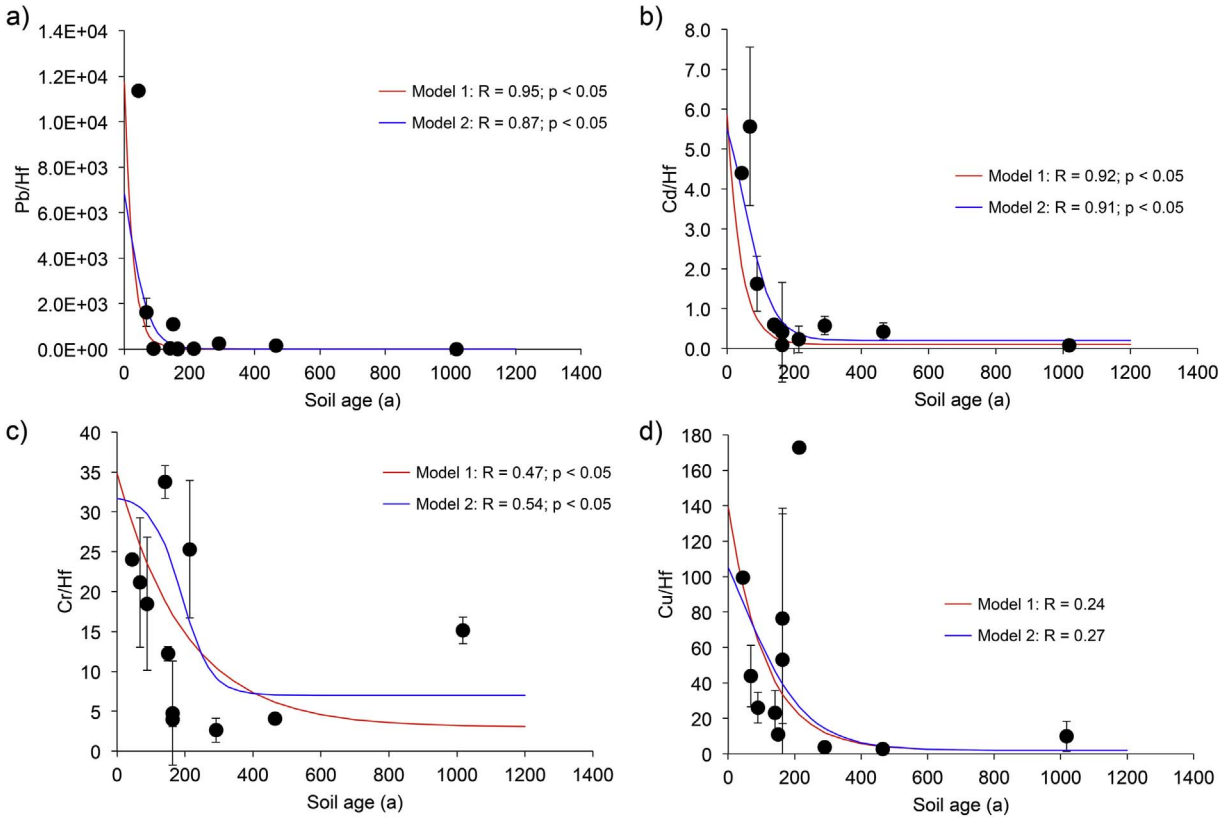

Fig. 8. Average ratios (± SD) of the trace metals a) Pb, b) Cd, c) Cr and d) Cu to the immobile element Hf in the weathered part of the soil profile as a function of time. The time trends were calculated using model 1 (Eq. (5)) and model 2 (Eq. (6)). Except for Cd, the values are normally distributed.

5. Discussion

The investigated juvenile soils on mine tailings reacted very rapidly and distinctly, similar to Alpine soils of young surfaces (Mavris et al., 2010). It is known that pH may exhibit very strong spatial variability (e.g., Papritz and Flühler, 1991). This is not that surprising as the neutralising and acid potential of mine tailings may strongly vary within the micro-meter scale (Redwan et al., 2017). Despite this spatial variability, a distinct decrease with time was measured. A sharp decrease in the pH at the beginning of soil formation is typical (Mavris et al., 2010; Sauer et al., 2009). Carbonate (present in low amounts) is very easily leached. The oxidation of sulphur in the presence of water strongly accelerates soil acidification. Because carbonate-free soils have a low buffering capacity, the acidification is even more pronounced. As reported by Dahms et al. (2012), chemical weathering proceeds rapidly in humid and cool alpine climates. Furthermore, their results show that chemical weathering clearly decreased with increasing age of the soil. In the case of Mont Chemin, the index-B values are in an absolutely similar range of Alpine soils after approximately 1000 years (near 0.4; Dahms et al., 2012). Elemental leaching at the Mont Chemin site occurs fast which is also due to the high rock fragment content and porosity (or relatively low density; Table 2). Zhen et al. (2015) showed that increased bulk density and silt and clay content reduce the average soil pore water velocity and dispersivity coefficient, thus extending the solute penetration time and thus leaching from mine wastes. Within the first few hundreds of years of soil development (Mont Chemin), despite some differences in the chemistry of the parent material, increasing concentrations of pedogenetically-formed phases such as Al(o), Fe(o) or Mn(o) can be detected with time (similarly as reported in Dahms et al., 2012). Consequently, chemical weathering processes seem to proceed very fast in the investigated environment. In addition, org. C and N accumulate with time in the soils. The exceptionally low C/N ratio in some subsoils can however not be explained well. An explanation for the very low C/N ratio particularly in the deeper soil horizons, might be due to the exceptionally high accumulation of nitrate beneath the active rooting zone. Due to the presence of a high amount of mostly positively charged Fe-oxides, NO_3^--N might be particularly well adsorbed. As observed by Eick et al. (1999), acid subsoils high in variable charge minerals may have the potential to retard NO_3 leaching.

Most of the trace metals presented here also reacted intensively at the beginning of exposure. This reaction strongly decreased with time. Although the starting content of trace metals in the soil or mine tailing material was not everywhere equal (which would be necessary for an unbiased observation over time), a temporal trend for all elements was detected. By normalising the trace element to an immobile element, the spatial variability was minimised allowing for the observation of a time trend. To a certain extent, the detected trends are consistent with the findings of Kim and Hyun (2015), which showed that the concentrations of aqueous Cu, Zn and Cd were quickly reduced with the number of leaching steps of abandoned mine sites. However, the reduction of Pb was less substantial. This reaction pattern follows a biphasic leaching model by allocating a large rapidly leaching fraction for Cu, Zn and Cd and an almost negligible fraction for Pb and As. According to Kim and Hyun (2015), the amount of eluted mass from the column was residence time-limited and affected by seepage conditions. In general, the solubility of these elements is pH-dependent and, for As, also a function of the redox-conditions (Moldovan and Hendry, 2005).

In sulphur deposits, the oxidative weathering process and reaction

Table 7
Correlation analysis with the trace metals Cr, Cu, Cd and Pb as dependent variables and pH, org. C, Mn_o, Fe_o, Fe_d, Al_o, Al_d, Fe_{d-o}, and Al_{d-o} content as independent variables (n = 35). For the multiple linear regression model only pH, org. C, Fe_o, Fe_d, and Al_d were used as independent variables. The multiple linear regression has the form: log [trace metal] = intercept + a_1pH + a_2 [log (org. C)] + a_3 [log(Fe_o)] + a_4 [log(Fe_d)] + a_5 [log(Al_d)].

Correlation coefficients R	Cr	Cu	Cd	Pb
pH	− 0.05	0.27	0.38*	0.03
Corg	− 0.62**	− 0.03	− 0.44**	− 0.36*
Mn(o)	0.22	− 0.04	0.22	0.10
Fe(o)	0.22	0.07	0.22	0.15
Fe(d)	0.08	0.39*	− 0.08	− 0.26
Al(o)	0.28	− 0.06	0.04	− 0.03
Al(d)	− 0.18	0.20	− 0.58**	− 0.49**
Fe(d-o)	− 0.10	0.41*	− 0.09	− 0.28
Al(d-o)	− 0.23	0.22	− 0.61**	− 0.51**

Multiple regression		Regression coefficient (a)	Error probability (p)	R^2	Standardised R^2
Element	Variable				
log(Cr)	Intercept	2.270	0.192		
	pH	− 0.034	0.022		0.062
	log [org. C (g/kg)]	− 0.175	0.044		0.390
	log [Fe_o (g/kg)]	0.062	0.065		0.038
	log [Fe_d (g/kg)]	− 0.047	0.080		0.017
	log [Al_d (g/kg)]	− 0.056	0.145		0.005
				0.462**	Σ0.513
log(Cu)	Intercept	0.153	0.800		
	pH	0.139	0.092		0.078
	log [org. C (g/kg)]	− 0.106	0.184		0.011
	log [Fe_o (g/kg)]	− 0.405	0.270		0.121
	log [Fe_d (g/kg)]	0.741	0.334		0.319
	log [Al_d (g/kg)]	0.455	0.605		0.025
				0.308*	Σ0.553
log(Cd)	Intercept	1.627	0.630		
	pH	0.075	0.072		0.023
	log [org. C (g/kg)]	− 0.126	0.145		0.016
	log [Fe_o (g/kg)]	0.490	0.213		0.184
	log [Fe_d (g/kg)]	− 0.050	0.263		0.002
	log [Al_d (g/kg)]	− 1.674	0.476		0.353
				0.555**	Σ0.577
log(Pb)	Intercept	7.754	1.452		
	pH	− 0.168	0.166		0.028
	log [org. C (g/kg)]	− 0.295	0.334		0.020
	log [Fe_o (g/kg)]	1.115	0.491		0.225
	log [Fe_d (g/kg)]	− 0.844	0.607		0.102
	log [Al_d (g/kg)]	− 2.848	1.098		0.242
				0.439**	Σ0.617

* Error probability < 0.05.
** Error probability < 0.01.

with water is often the main cause of soil and water acidification and the translocation of major amounts of trace metals (Egli et al., 2011a). Seepage water from coal and metal mines exhibits high levels of sulphuric acid and trace metals. In this respect, metal-disulphides are particularly problematic (metal mono-sulphides cause less acidification of soils and water). Conditions are favourable for the production of acid mine drainage at Mont Chemin. Ansermet (2001) reports that pyrite (FeS_2) is present in the fluorine and galena veins of Mont Chemin. This is also confirmed with our measurements (Table 6). Therefore, strongly acidic mine waters must occur close to these types of veins (Egli et al., 2011b). In addition, coniferous litter may accelerate these processes due to its potential to produce acids during decay.

As soon as soils develop some humic substances and oxyhydroxides, they can efficiently capture metals over sorption processes when seepage water flows through them (Pfeifer et al., 2004). However, mobilisation, transport, immobilisation and remobilisation of trace metals is a complex process and, of course, depends on the element. In addition, young soils that have developed on mine wastes have low clay contents and moderate amounts of organic matter. Consequently, these sorption processes are insufficient in such soils, at least in the early stage of soil development. This is also shown by the correlation and multiple regression analyses. Usually, total Pb, Cu, Cr and Cd contents correlate positively with soil organic matter (Egli et al., 2010). This means that such components are often retained through adsorption processes by organic matter. If highly soluble compounds are however present (e.g. phenols) then these metals may also be translocated to greater depths (Egli et al., 2010). The negative correlation of Pb, Cu, Cr and Cd with organic C (Table 7) seems to indicate that at least at the beginning of soil formation a part of these metals (Cr, Cd, Pb) is leached either with soluble organic compounds or was not retained enough at

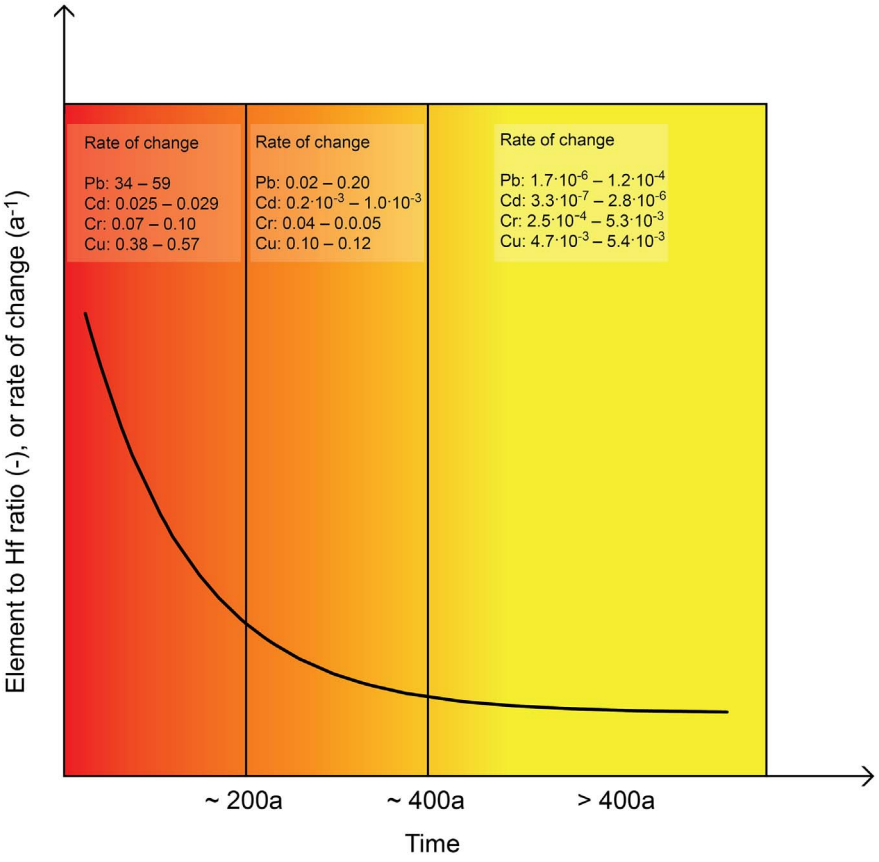

Fig. 9. Schematic arrangement of rates of change (element to Hf-ratio) with time.

Table 8
Classification of the reactivity of Pb and Cu (based on Figs. 8 and 9) considering the long-term chemical behaviour and weathering.

Class	Duration since last exploitation
Strongly reactive	0–200 years
Moderately reactive	200–400 years
Weakly reactive	> 400 years
Unknown	Unknown

the initial stages of soil formation because not enough organic carbon (or not in the necessary chemical form to retain these elements) was present.

Because large part of the crystalline Fe- and Al-oxyhydroxides in the soils has a positive charge at such soil pH-values, their retention capability of the investigated trace metals is quite limited. Metal adsorption strength to nanohematite at pH 6.0 would increase with metal electronegativity: Pb > Cu > Zn ~ Cd (Grover et al., 2011). At lower pH values, however, adsorption is generally strongly reduced. The mostly negative relation of Al(d-o) and Fe(d-o) with the investigated trace metals underpins such a mechanisms: with time trace metals are more and more leached and not retained effectively by Fe- and Al-oxyhydroxides. The chosen multiple regression explains reasonably well the characteristics of the trace elements. Soil acidity, organic matter and oxyhydroxides are the main drivers (Egli et al., 1999), although a potential multicollinearity among the Fe and Al species may exist. In our case, weakly crystalline manganese does not (yet) have any importance. The best multiple linear fit is obtained when pH, org. C, Fe_o, Fe_d and Al_d are used as independent variables. In our case, the geochemistry of Cr seems to be governed to a great extent by soil organic matter (Table 7; see standardised R^2). The content of Cu, Cd and Pb, however, depends more on the presence and type of oxyhydroxides (Table 7).

The knowledge and data of small mines are very often strongly limited. In most cases, the environmental impact of such mines is considered either to be small due to the rather small extent of the contaminated zone and the fact that they are often situated in a remote area at high altitude (Pfeifer et al., 2007). It is, nonetheless, obvious that these sites are strongly contaminated and that they exhibit a potential ecological as well as human health risk. Furthermore, coal mining activities are inevitably connected with the production of acidic drainage and airborne compounds such as fly ash and bottom ash with high metal contents. Soil is the dominant sink for trace elements discharged from this type of anthropogenic source (Pandey et al., 2016).

From a legal point of view, the regulations regarding soil contamination, risks and sanitation are quite rigorous in Switzerland (Mailänder and Hämmann, 2005). Detailed risk evaluation methods exist to estimate the risk level for contaminated sites and derive suitable methods to reduce the potential uptake of trace metals. These concepts are, however, not valid for forested areas. The regulations consider only agricultural land and urban surfaces. Acid mine drainages are a severe problem for the environment. In principle, this problem can be addressed in the planning phase of a mining site. Although mine locations are determined based on the mineral occurrences, advance planning and analysis could avoid implementation of mine facilities in locations where failure or leaks would cause too much damage to natural resources. Watershed-scale transport modelling could help determine facility locations, or determine in advance that the mine should not be constructed due to the risk to downstream resources (Myers, 2016). To delimit risk zones of already existing mine dumps, models can help to separate the waste material into different clusters according to the concentration of trace elements in the waste. This helps to identify zones with different levels of risk (e.g., to agriculture production; Romero et al., 2015).

In our investigation area (Mont Chemin), very high concentrations of Pb, Cu, etc., were measured in the soil. The contaminated zones are dispersed (Fig. 3), and some hot spots are evident close to the mining

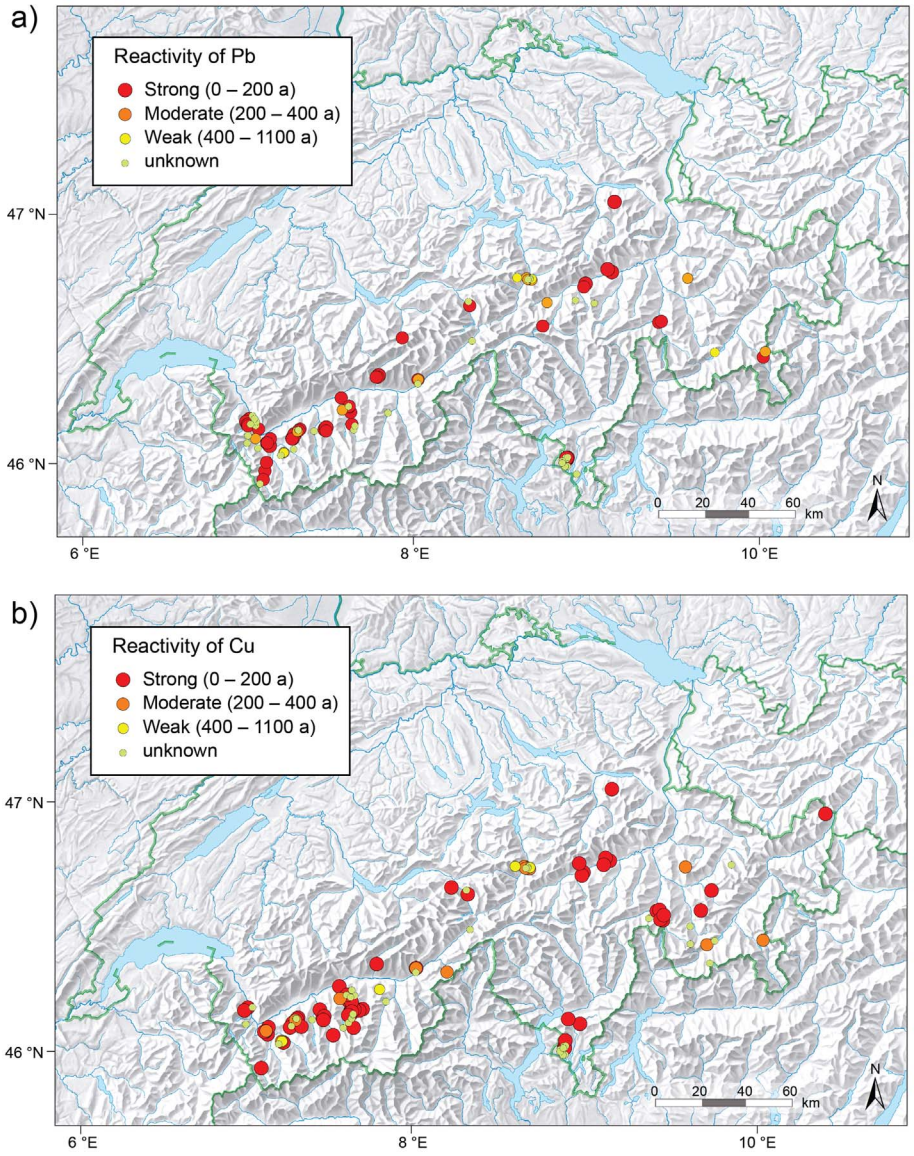

Fig. 10. Classification of former mining sites in Switzerland regarding their reactivity for a) Pb and b) Cu. Reproduced by permission of swisstopo (BA17094).

activities. Some of these hot spots and contaminated areas are close to pastureland. Furthermore, some drinking water sources (although not intensively used here) are in close proximity to these sites. Many similar mining sites exist in Switzerland. Due to the very low number of investigations, no chemical data about soil contamination are available. A direct risk assessment is therefore not possible or at least not easily performed. Chemical processes, such as sorption and precipitation, result in the long-term natural demobilisation of inorganic pollutants (Förstner and Grathwohl, 2003). Using the chronosequence approach, the weathering and leaching behaviour could be derived (Figs. 8 and 9). Three general categories can be distinguished: strongly reactive, moderately reactive and weakly reactive (Fig. 9, Table 8) sites. Using this approach, an extrapolation to the entirety of Switzerland was rendered possible by using the SGTK database. By selecting mining activities over time, used minerals (and related chemical elements: in this case, Pb and Cu), and by considering a similar geology to our investigation site (Mont Chemin), an evaluation of the reactivity of abandoned mining sites in Switzerland was enabled (Fig. 10). In addition to the above-mentioned three categories of reactivity, a fourth category was considered: at some sites, no precise information about the abandonment was available (Fig. 10). Most of the abandoned mining sites in Switzerland have a relatively young soil age. Consequently, the reactivity of most sites is still very high. Some of the highly reactive sites are even within groundwater protection areas and close to either drinking water wells or sources. The duration of reactivity also depends on the amount of material that has been dumped. The mined ores often contain sulphides (such as pyrite) that react on the surface with water and oxygen to produce sulphuric acid (Förstner and Grathwohl, 2003; Hirner et al., 2000; Lawrence et al., 1997; Lin et al., 2007). This process strongly increases local acidity, which is the main driver for trace metal mobility. The considered sites in Switzerland are, however, all small and restricted to very local outcrops. From this point of view, they are moderately comparable. Although the used concept enables a spatialisation, it should be emphasised that it only gives a rough estimate and that it is a strong simplification of reality. However, it enables the detection of sites with high potential risk for the environment. This estimated risk can then be further investigated in situ.

6. Conclusions

Using a chronosequence approach, metal leaching at the

investigation area of Mont Chemin could be traced back over a time period of approximately 1000 years. Although the soil and parent material show some variability, relatively clear time-trends could be delineated. The elemental leaching effect was particularly pronounced during the first 200 years after abandonment of the sites. With increasing time, however, the rate of change and subsequent leaching strongly diminished. Particularly at the beginning of soil formation, soil organic carbon and the present oxyhydroxides do not have a sufficient capacity to retain trace metals such as Cr, Cu, Cd and Pb. This general observation over time allowed an extrapolation to former (small) mining sites in the Swiss Alps. Most of these sites were abandoned during the last two centuries and can therefore be considered as still highly reactive. A detailed risk assessment cannot directly be derived and would require further in situ investigation.

Acknowledgements

This research was supported by the Swiss Government Excellence Scholarship (2016.0646/Brazil/OP) for Raquel de Castro Portes. We would like to thank Peter Kühn (University of Tübingen), Rita Mögenburg (University of Tübingen) and Andreas Jallas (ETHZ) for their support with the preparation of the thin sections and Lukas Martin (ETHZ) for the SEM-EDS analyses. We are, furthermore, indebted to unknown reviewers for their helpful comments on an earlier version of the manuscript.

References

Ansermet, S., 2001. Le Mont Chemin. Mines and Minerals of the Swiss canton of Valais. Mines et Minéraux du Valais; in French. Musée Cantonal d'Histoire Naturelle, Sion (éditions pillet, Saint-Maurice).
Arefieva, O.D., Shapkin, N.P., Gruschakova, N.V., Prokuda, N.A., 2016. Mine water: chemical composition and treatment. Water Pract. Technol. 11, 540–546.
BAFU (Bundesamt für Umwelt), 2007. Hydrologic atlas of Switzerland (in German; Hydrologischer Atlas der Schweiz HADES). Swisstopo, Wabern.
Bech, J., Abreau, M.M., Chon, H.T., 2017. Preface special issue CATENA: Reclamation of mining soils, part II. Catena 148, 1–2.
Borggaard, O.K., 1988. Phase indication by selective dissolution techniques. In: Stucki, J.W., Goodman, B.A., Schwertmann, U. (Eds.), Iron in Soils and Clay Minerals. D. Reidel Publishing Company, Dordrecht, pp. 83–89.
Bortnikova, S.B., Olenchenko, V.V., Gaskova, O.L., Chernii, K.I., Devyatova, A.Y., Kucher, D.O., 2017. Evidence of element emission during the combustion of sulfide-bearing metallurgical slags. Appl. Geochem. 78, 105–115.
Bronk Ramsey, C., 2001. Development of the radiocarbon calibration program. Radiocarbon 43, 355–363.
Bronk Ramsey, C., 2009. Bayesian analysis of radiocarbon dates. Radiocarbon 51, 337–360.
Candeias, C., Melo, R., Ávila, P.F., da Silva, E.F., Salgueiro, A.R., Teixeira, J.P., 2014. Heavy metal pollution in mine–soil–plant system in S. Francisco de Assis – Panasqueira mine (Portugal). Appl. Geochem. 44, 12–26.
Coulthard, T.J., Macklin, M.G., 2003. Modeling long-term contamination in river systems from historical metal mining. Geology 31, 451–454.
Dahms, D., Favilli, F., Krebs, R., Egli, M., 2012. Soil weathering and accumulation rates of oxalate-extractable phases from alpine chronosequences of up to 1 Ma in age. Geomorphology 151–152, 99–113.
Dennis, I.A., Macklin, M.G., Coulthard, T.J., Brewer, P.A., 2003. The impact of the October–November 2000 floods on contaminant metal dispersal in the River Swale catchment, North Yorkshire, UK. Hydrol. Process. 17, 1641–1657.
Dudka, S., Adriano, D.C., 1997. Environmental impacts of metal ore mining and processing: a review. J. Environ. Qual. 26, 590–602.
Duruibe, J.O., Ogwuegbu, M.O.C., Egwurugwu, J.N., 2007. Heavy metal pollution and human biotoxic effects. Int. J. Phys. Sci. 2, 112–118.
Egli, M., Fitze, P., Oswald, M., 1999. Changes in heavy metal contents in an acidic forest soil affected by depletion of soil organic matter within the time span 1969–1993. Environ. Pollut. 105, 367–379.
Egli, M., Sartori, G., Mirabella, A., Giaccai, D., Favilli, F., Scherrer, D., Krebs, R., Delbos, E., 2010. The influence of weathering and organic matter on heavy metals lability in silicatic, Alpine soils. Sci. Total Environ. 408, 931–946.
Egli, M., Krebs, R., Berger, R., Rieben, S., Bollinger, R., Tissières, P., 2011a. Investigations of Agriculturally Used Areas on Sites Polluted With Trace Metals Deriving From Former Mining Sites of the Mont Chemin (in German; Untersuchung Landwirtschaftlich Genutzter flächen auf Schwermetallverunreinigten Standorten Ehemaliger Minen am Mont Chemin). Département des Transports, de l'équipement et de l'environnement; Service de la protection de l'environnement, Canton du Valais, Sion.
Egli, M., Leumann, A., Krebs, R., 2011b. Heavy metals contamination in soils near formerly mined metal ores of the Mont Chemin. BGS Bull. 31, 51–56.
Eick, M.J., Brady, W.D., Lynch, C.K., 1999. Charge properties and nitrate adsorption of some acid southeastern soils. J. Environ. Qual. 28, 138–144.
Förstner, U., Grathwohl, P., 2003. Engineering Geochemistry: Decay and Retention, Stabilisation of Wastes (in German; Ingenieurgeochemie: Natürlicher Abbau und Rückhalt, Stabilisierung von Massenabfällen). Springer Verlag, Berlin.
Garcia-Guinea, J., Harffy, M., 1998. Bolivian mining pollution; past present and future. Ambio 27, 251–253.
Grover, V.A., Hu, J., Engates, K.E., Shipley, H.J., 2011. Adsorption and desorption of bivalent metals to hematite nanoparticles. Environ. Toxicol. Chem. 31, 86–92.
Guénette-Beck, B., Meisser, N., Curdy, P., 2009. New insights into the ancient silver production of the Wallis area, Switzerland. Archaeol. Anthropol. Sci. 1, 215–229.
Harden, J.W., 1982. A quantitative index of soil development from field descriptions: examples from a chronosequence in central California. Geoderma 28, 1–28.
Hirner, A.V., Rehage, H., Sulkowski, M., 2000. Environmental Geochemistry. Origin, Mobility and Analysis of Pollutants in the Pedosphere (in German; Umweltgeochemie. Herkunft, Mobilität und Analyse von Schadstoffen in der Pedosphäre). Steinkopff, Darmstadt.
Hitz, C., Egli, M., Fitze, P., 2002. Determination of the sampling volume for representative analysis of alpine soils. Z. Pflanzenernähr. Bodenkd. 165, 326–331.
Huff, L.C., 1976. Migration of lead during oxidation and weathering of lead deposits. In: Sheridan, D.M., Marsh, S.O., Mrose, M.E., Taylor, R.B. (Eds.), Mineralogy and Geology of the Wagnerite Occurrence on Santa Fe Mountain Front Range, Colorado. Geological Survey Professional Paper 955 United States Government Printing Office, Washington, pp. 21–24.
Hugi, E., Huttenlocher, H.F., Gassmann, F., Fehlmann, H., Ladame, G.C., Hügi, T., Wohlers, J., 1948. Die Magnetitlagerstätten. Die Eisen- und Manganerze der Schweiz, Bd 4. Beitr. Geol. der Schweiz Geotech Ser 13 (4), 1–116 Kümmerli & Frey, Bern.
IUSS Working Group WRB, 2014. International soil classification system for naming soils and creating legends for soil maps. In: World Reference Base for Soil Resources 2014. World Soil Resources Reports 106 FAO, Rome.
Keim, M.F., Markl, G., 2015. Weathering of galena: Mineralogical processes, hydrogeochemical fluid path modeling and estimation of the growth rate of pyromorphite. Am. Mineral. 100, 1584–1594.
Kim, J., Hyun, S., 2015. Nonequilibrium leaching behavior of metallic elements (Cu, Zn, As, Cd, and Pb) from soils collected from long-term abandoned mine sites. Chemosphere 134, 150–158.
Kronberg, G.I., Nesbitt, H.W., 1981. Quantification of weathering of soil chemistry and soil fertility. J. Soil Sci. 32, 453–459.
Lawrence, J.R., Kwong, Y.T.J., Swerhone, G.D.W., 1997. Colonization and weathering of natural sulfide mineral assemblages by *Thiobacillus ferrooxidans*. Can. J. Microbiol. 43, 178–188.
Lichter, J., 1998. Rates of weathering and chemical depletion in soils across a chronosequence of Lake Michigan sand dunes. Geoderma 85, 255–282.
Lin, C., Wu, Y., Lu, W., Chen, A., Liu, Y., 2007. Water chemistry and ecotoxicity of an acid mine drainage-affected stream in subtropical China during a major flood event. J. Hazard. Mater. 142, 199–207.
Mailänder, R.A., Hämmann, M., 2005. Handbook – Risk Assessment and Measures for Polluted Soils (in German; Handbuch – Gefährdungsabschätzung und Massnahmen bei schadstoffbelasteten Böden – Gefährdungsabschätzung Boden. Vollzug Umwelt). Bundesamt für Umwelt, Wald und Landschaft, Bern.
Mavris, C., Egli, M., Plötze, M., Blum, J., Mirabella, A., Giaccai, D., Haeberli, W., 2010. Initial stages of weathering and soil formation in the Morteratsch proglacial area (Upper Engadine, Switzerland). Geoderma 155, 359–371.
McIntosh, J., 2006. Handbook to Life in Prehistoric Europe. Oxford University Press, New York.
McKeague, J.A., Brydon, J.E., Miles, N.M., 1971. Differentiation of forms of extractable iron and aluminium in soils. Soil Sci. Soc. Am. Proc. 35, 33–38.
Mizota, C., van Reeuwijk, L.P., 1989. Clay Mineralogy and Chemistry of Soils Formed in Volcanic Material in Diverse Climate Regions. vol. 2 International Soil Reference and Information Centre, Wageningen Soil Monograph.
Moldovan, B.J., Hendry, M.J., 2005. Characterizing and quantifying controls on arsenic solubility over a pH range of 1 − 11 in a uranium mill-scale experiment. Environ. Sci. Technol. 39, 4913–4920.
Myers, T., 2016. Acid mine drainage risks - a modeling approach to siting mine facilities in Northern Minnesota USA. J. Hydrol. 533, 277–290.
Navarro, M.C., Perez-Sirvent, C., Martinez-Sanchez, M.J., Vidal, J., Tovar, P.J., Bech, J., 2008. Abandoned mine sites as a source of contamination by heavy metals: a case study in a semi-arid zone. J. Geochem. Explor. 96, 183–193.
Pandey, B., Agrawal, M., Singh, S., 2016. Ecological risk assessment of soils contamination by trace elements around coal mining area. J. Soils Sediments 16, 159–168.
Papritz, A., Flühler, H., 1991. Spatial variability of soil chemical properties along transects between trees (investigation area Lägern) (in German; Räumliche Variabilität von bodenchemischen Grössen auf Transekten zwischen Bäumen (Beobachtungsfläche Lägern)). In: Pankow, W. (Ed.), Belastung von Waldböden. NFP, vol. 14. Zürich, Verlag der Fachvereine, pp. 125–136.
Pfeifer, H.-R., Gueye-Girardet, A., Reymond, D., Schlegel, C., Temgoua, E., Hesterberg, D.L., Chou, J.W., 2004. Dispersion of natural arsenic in the Malcantone watershed, Southern Switzerland: field evidence for repeated sorption–desorption and oxidation-reduction processes. Geoderma 122, 205–234.
Pfeifer, H.-R., Häussermann, A., Lavanchy, J.C., Halter, W., 2007. Distribution and behavior of arsenic in soils and waters in the vicinity of the former gold-arsenic mine of Salanfe, Western Switzerland. J. Geochem. Explor. 93, 121–134.
Plante, B., Benzaazoua, M., Bussière, B., 2011. Predicting geochemical behaviour of waste rock with low acid generating potential using laboratory kinetic tests. Mine Water Environ. 30, 2–21.
Redwan, M., Rammlmair, D., Nikonow, W., 2017. Application of quantitative mineralogy on the neutralization–acid potential calculations within μm-scale stratified mine tailings. Environ. Earth Sci. 76, 46. http://dx.doi.org/10.1007/s12665-016-6344-4.
Reimann, C., Arnoldussen, A., Finne, T.E., Koller, F., Nordgulen, Ø., Englmaier, P., 2007. Element contents in mountain birch leaves, bark and wood under different anthropogenic and geogenic conditions. Appl. Geochem. 22, 1549–1566.
Reimer, P.J., Bard, E., Bayliss, A., Beck, J.W., Blackwell, P.G., Bronk Ramsey, C., Buck, C.E., Cheng, H., Edwards, R.L., Friedrich, M., Grootes, P.M., Guilderson, T.P., Haflidason, H., Hajdas, I., Hatté, C., Heaton, T.J., Hoffmann, D.L., Hogg, A.G.,

Hughen, K.A., Kaiser, K.F., Kromer, B., Manning, S.W., Nui, M., Reimer, R.W., Richards, D.A., Scott, E.M., Southon, J.R., Staff, A.R.A., Turney, C., van der Plicht, J., 2013. IntCal13 and Marine13 radiocarbon age calibration curves 0–50,000 years cal BP. Radiocarbon 55, 1869–1887.

Romero, A., Gonzalel, I., Martin, J.M., Varquez, M.A., Ortiz, P., 2015. Risk assessment of particle dispersion and trace element contamination from mine-waste dumps. Environ. Geochem. Health 37, 273–286.

Sauer, D., Schülli-Mauer, I., Sperstad, R., Sørensen, R., Stahr, K., 2009. Albeluvisol development with time in loamy marine sediments of southern Norway. Quat. Int. 209, 31–43.

Shu, W.S., Ye, Z.H., Lan, C.Y., Zhang, Z.Q., Wong, M.H., 2001. Acidification of lead/zinc mine tailings and its effect on heavy metal mobility. Environ. Int. 26, 389–394.

Singh, A.N., Zeng, D.H., Chen, F.S., 2005. Heavy metal concentrations in redeveloping soil of mine spoil under plantations of certain native woody species in dry tropical environment, India. J. Environ. Sci. 1, 168–174.

Soil Survey Staff, 2014. Keys to Soil Taxonomy, 12th ed. United States Department of Agriculture Natural Resources Conservation Service, Washington, DC.

Strosnider, W.H., Nairn, R.W., Llanos, F.S., 2007. A legacy of nearly 500 years of mining in Potosí, Bolivia: acid mine drainage source identification and characterization. In: Proceedings America Society of Mining and Reclamation, pp. 788–803.

White, A.F., Brantley, S.L., 2003. The effect of time on the weathering of silicate minerals: why do weathering rates differ in the laboratory and field? Chem. Geol. 202, 479–506.

White, A.F., Hochella Jr., M.F., 1992. Surface chemistry associated with the cooling and subaerial weathering of resent basalt flows. Geochim. Cosmochim. Acta 56, 3711–3721.

Zhen, Q., Ma, W., Li, M., He, H., Zhang, X., Wang, Y., 2015. Effects of vegetation and physicochemical properties on solute transport in reclaimed soil at an opencast coal mine site on the Loess Plateau, China. Catena 133, 403–411.

Zhuang, P., McBride, M.B., Xia, H., Li, N., Li, Z., 2009. Health risk from heavy metals via consumption of food crops in the vicinity of Dabaoshan mine, South China. Sci. Total Environ. 407, 1551–1561.